Photochemical & Photobiological Sciences

PAPER

View Article Online
View Journal | View Issue

Open Access Article. Published on 08 December 2017. Downloaded on 1/20/2026 5:10:44 AM.
This article is licensed under a Creative Commons Attribution 3.0 Unported Licence.

Check for updates

Cite this: *Photochem. Photobiol. Sci.*, 2018, **17**, 213

Visible-light-driven two-way photoisomerization of 1-(1-pyrenyl)-2-(2-quinolyl)ethylene in neutral and protonated forms†

Mikhail F. Budyka * and Vitalii M. Li

Received 26th September 2017,
Accepted 8th December 2017

DOI: 10.1039/c7pp00359e

rsc.li/pps

Diarylethylenes with large π-systems often lose their photochemical activity (the size effect). 1-(1-Pyrenyl)-2-(2-quinolyl)ethylene (1P2QE), despite having a large conjugated π-system of 28 electrons, undergoes two-way reversible *trans–cis* photoisomerization both in the neutral and protonated forms with quantum yields as high as 0.13–0.83. For the neutral 1P2QE, experimental data and quantum-chemical calculations indicate a diabatic (nonadiabatic) reaction mechanism. Due to high photoisomerization quantum yields and the long-wavelength absorption band at 340–460 nm and 390–560 nm for the neutral and protonated compounds, respectively, 1P2QE can be used as a molecular photoswitch that is sensitive to visible light.

1. Introduction

Photoisomerization is one of the fundamental reactions in photochemistry. Photoisomerization of retinal is a primary photochemical step in the signal transduction cascade of vision.[1,2] Photoisomerization of stilbene and azobenzene derivatives, which are the most widespread photochromes, is a functioning mechanism of many photonic molecular switches and logic gates.[3–6] For example, by photoisomerization of different diarylethylenes (DAEs), it is possible to perform the functions of different molecular logic gates.[7,8]

A molecular photonic switch is defined as a compound that can reversibly transform between two (or more) states under light irradiation. There are two main parameters that characterize the photochemical properties of a photonic switch: the region of spectral sensitivity and the photoisomerization quantum yield. Spectral sensitivity is defined by the absorption spectrum of a photochrome that is used as a photonic switch. Commonly, photoswitches, being rather small molecules, absorb light in the UV region (at least, one of the photochrome isomers); however, for many applications, the visible region is more suitable, since it reduces the damage from UV irradiation of the material.[9] Therefore, the possibility of switching the photochrome using visible light has attracted increasing attention.[10–13]

There are several mechanisms of spectral tuning. In nature, the spectral sensitivity of the retinal photochrome is tuned over a broad wavelength range by environmental variation since the retinal absorption spectrum depends on interaction with the opsin protein, to which retinal is bound (on the polarity of the retinal binding pocket of rhodopsin, on proximity of the counter ion).[1,2] Owing to this dependence, the same retinal photochrome provides color vision across the visible spectrum.

In azobenzene-based photoswitches, the spectrum is tuned by introducing electron-donating and/or electron-withdrawing substituents, which can significantly affect the π–π* and n–π* absorption bands (and simultaneously, the thermal stability).[9]

The most general mechanism of spectral tuning, which is used for designing visible-light photoswitches, is a decrease in the photochrome HOMO–LUMO (highest occupied – lowest unoccupied molecular orbital) gap that is achieved by extending the conjugated π-system of the photochrome.[9] A smaller HOMO–LUMO gap produces a red-shifted absorption spectrum. However, photochrome, with a large π-system, often loses photochemical activity that prevents its exploitation as a photoswitch despite possessing the necessary absorption spectrum.

For example, on going from stilbene to 2-styrylnaphthalene (SN), the DAE π-system increases from 14 to 18 π-electrons and the *trans* → *cis* photoisomerization quantum yield (ϕ_{tc}) drops from ~0.5 to 0.12.[14–16] The further increase in the π-system by

Institute of Problems of Chemical Physics, Russian Academy of Sciences, pr. Akademika Semenova 1, Chernogolovka, Moscow region, 142432, Russian Federation. E-mail: budyka@icp.ac.ru

† Electronic supplementary information (ESI) available: Synthetic details, experimental and calculated absorption spectra, fluorescence decay profile, dependence of fluorescence spectra on excitation wavelength, principal component analysis, transition energies, nature and oscillator strengths of the lowest excited singlet states calculated by TDDFT/B3LYP, calculated optimized geometries in the S_0 and S_1 states, minimal energy paths calculated by PM3 and PM3-CI (2 × 2). See DOI: 10.1039/c7pp00359e

Open Access Article. Published on 08 December 2017. Downloaded on 1/20/2026 5:10:44 AM.
This article is licensed under a Creative Commons Attribution 3.0 Unported Licence.

4 electrons gives rise to 2-styrylanthracene (SA, 22 electrons), at which the ϕ_{tc} value reduces practically to zero.[17,18] Since the *cis*-isomer remains reactive (the *cis* → *trans* photoisomerization quantum yield ϕ_{ct}>0), the photochemical properties of SA are characterized as a 'one-way' *cis* → *trans* photoisomerization reaction. The sharp ϕ_{tc} decrease when the π-system exceeds some threshold size, which is the so-called 'size effect', is explained by the change in the reaction mechanism from diabatic (nonadiabatic) to adiabatic: upon excitation of the *cis*-isomer, the system 'slides' along the excited-state potential energy surface (PES) to the *trans*-isomer (adiabatic mechanism) passing the *perp*-conformer (phantom state), where it could branch between *trans*- and *cis*-isomers (diabatic mechanism, see below). When the *trans*-isomer is excited, the energy is localized on the large aromatic nucleus, which increases the barrier on the excited state PES and prevents twisting to the *perp*-conformer (and further to the *cis*-isomer).[19] One-way adiabatic *cis*–*trans* photoisomerization (in the singlet-excited state) is also characteristic for 1-styrylpyrene (SP), which has 24 π-electrons.[20]

According to the functioning mechanism, azobenzene derivatives and DAEs are *E*/*Z* (*trans*/*cis*) photoswitches. In contrast to azobenzene derivatives, DAEs are rarely used as photoswitches despite their advantages, for example, they have thermally stable isomers separated by a large barrier in the ground (S_0) state that results in fully photo-driven switching.

X. Guo *et al.*[11] have noted that surprisingly little effort has been devoted to developing visible-light-triggered "non-azo" *E*/*Z* photoswitches. They have designed bis(dithienyl)dicyanoethene (4TCE) with absorption bands in the visible region, which is capable of isomerizing under visible light.[11,21] An interesting property of 4TCE is that *E*/*Z* photoswitching operates by multiplicity-exclusive pathways: *trans*-to-*cis* isomerization only occurs in the S_1 state, whereas *cis*-to-*trans* isomerization occurs in the T_1 state. Moreover, the photoisomerization quantum yields vary with excitation wavelength; for example, ϕ_{ct} is negligible at 530 nm and increases to 0.05 at 420 nm.[21]

Earlier, we have studied the size effect in a series of aza-DAEs – derivatives of 2-styrylquinoline (SQ). Upon stepwise addition of the benzene rings to the styryl fragment, we obtained 1-(1-naphthyl)-2-(2-quinolyl)ethylene 1N2QE,[22] 1-(2-naphthyl)-2-(2-quinolyl)ethylene 2N2QE[22] and 1-(9-anthryl)-2-(2-quinolyl)ethylene 9A2QE[23] (Scheme 1, only s-*trans* and s-*cis* conformers relative to the vinyl-quinoline single bond are shown; depending on the structure of the aryl group, the corresponding s-*trans* and s-*cis* conformers relative to the vinyl-aryl single bond can also exist). In this series, the π-system size increases from 18 π-electrons (SQ) to 26 π-electrons (9A2QE). In accordance with this, the long-wavelength absorption band (LWAB) in the row of SQ–2N2QE–9A2QE is bathochromically shifted in the sequence of 340–348–393 nm for the *trans*-isomers and 272–327–390 nm for the *cis*-isomers. In the same row, the photoisomerization quantum yield changes as 0.27–0.39–0.33 for the ϕ_{tc} and 0.38–0.54–0.40 for the ϕ_{ct}, *i.e.*, all these compounds are photoactive and undergo two-way photoisomerization. Therefore, in this series of aza-DAEs, the threshold size of the π-system is more than 26 electrons.

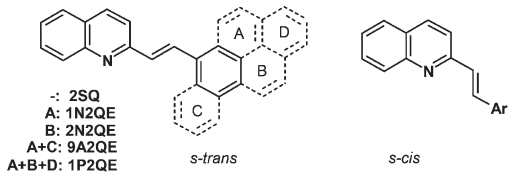

Scheme 1 Structure of 2-styrylquinoline and its annelated derivatives (s-*trans* and s-*cis* conformers relative to the vinyl-quinoline single bond are shown).

The next compound in this series where the size effect could manifest itself is 1-(1-pyrenyl)-2-(2-quinolyl)ethylene (1P2QE), which has 28 π-electrons, Scheme 1. This compound was previously synthesized,[24] however, its photochemical properties have not been studied. The lack of the size effect observed previously makes the pyrene-substituted system a good candidate for pushing the spectral response into the visible region.

An additional advantage of aza-DAEs in comparison to all-carbon analogues is that they have an extra channel for spectral tuning: under protonation, their absorption spectra are red-shifted, widening the spectral sensitivity region.[22,23] The effect of the nitrogen heteroatom on the photochemical properties of 1,2-diarylethenes has been previously studied.[25]

Considering the above discussion, in the present paper, we studied the photochemical properties of 1P2QE. In contrast to SP, 1P2QE proved to be photoactive and underwent two-way photoisomerization in the neutral and protonated forms with quantum yields of 0.13–0.83 under visible light irradiation.

2. Experimental section

1P2QE was prepared from quinaldine and 1-pyrenecarboxaldehyde by slightly modifying the previously described microwave-assisted solvent-free technique[26] (see details in the ESI†).

All studies were carried out in air-saturated solutions in ethanol at room temperature. The protonated form was obtained *in situ* by adding the required amount of HCl. Quartz cells with an optical path length of l = 1 cm were used. Electronic absorption spectra were recorded on a Specord M-400 spectrophotometer; emission spectra were recorded on a PerkinElmer LS-55 spectrofluorimeter. Fluorescence quantum yields were measured using a dilute alcohol solution of anthracene as a standard (with a fluorescence quantum yield of 0.3 (ref. 27)), with a measurement accuracy of 15%. Fluorescence lifetimes were measured by a PicoQuant GmbH instrument, using the single photon counting method.

A light-emitting diode LED-260 (emitting wavelength 260 nm, full width at half maximum FWHM = 12 nm) and a DRSh-500 high-pressure mercury lamp were used as sources of UV and visible light. The spectral lines at 313, 365, 405, 436 and 546 nm were isolated with a set of glass filters from

 This journal is © The Royal Society of Chemistry and Owner Societies 2018

Open Access Article. Published on 08 December 2017. Downloaded on 1/20/2026 5:10:44 AM.
This article is licensed under a Creative Commons Attribution 3.0 Unported Licence.

Elektrosteklo. Light intensity of (1–5) × 10^{-9} Einstein cm^{-2} s^{-1} was measured by a ferrioxalate actinometer. Photoisomerization quantum yields were calculated by numerical solution of a set of differential equations and averaged in several experiments; error did not exceed 20%. All experiments were performed in a darkroom under red light.

2.1 Quantum-chemical calculations

Geometry optimizations were performed using the Gaussian 09 program package.[28] The structures of the compounds in the ground state were calculated with full optimization of the geometrical parameters using semiempirical PM3 and DFT B3LYP/6-31G* methods. The optimized structures corresponded to the minima at the potential energy surfaces and had no imaginary frequencies in the vibrational spectra. The absorption spectra were calculated by the time-dependent (TD) B3LYP/6-31G* method using ground-state geometry optimized at the B3LYP/6-31G* level. In the S_1 state, optimization of the geometrical parameters was performed by TD B3LYP/6-31G* and PM3 with configuration interaction PM3-CI(2 × 2). Minimal energy paths on the PESs (reaction profiles) were calculated by the PM3 (the S_0 state) and PM3-CI(2 × 2) methods (the S_1 state).

3. Results and discussion

Fig. 1 shows the UV/Vis absorption spectra of 1P2QE in the neutral and protonated forms; the spectra of the *trans*-isomers are experimental, while the spectra of the *cis*-isomers are calculated by Fischer's method.[29] The LWAB of the neutral *trans*-isomer has a maximum at 387 nm (ε = 3.92 × 10^4 L mol^{-1} cm^{-1}). For the *cis*-isomer, a hypsochromic shift of the LWAB (characteristic for the DAEs) up to 364 nm is observed and accompanied by a decrease in intensity (ε = 2.36 × 10^4 L mol^{-1} cm^{-1}) in comparison with the *trans*-isomer.

It should be noted that pyrene itself has a very characteristic absorption spectrum with a well-defined vibrational structure (Fig. S3 in the ESI†).[30] Due to the planar structure and participation of the pyrene nucleus in π-conjugation, in *E*-1P2QE (as well as in *E*-SP[20]), the local pyrene ($S_2 \leftarrow S_0$) transition in the region of 320–340 nm is practically masked by the $S_1 \leftarrow S_0$ transition of the 1P2QE molecule as a whole.

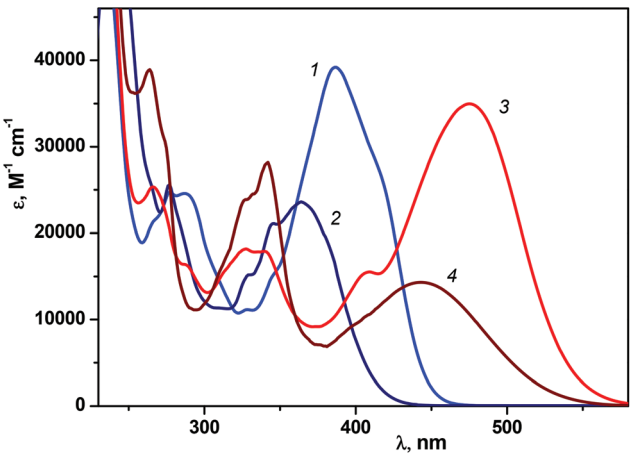

Fig. 1 Absorption spectra (in ethanol) of 1P2QE: neutral (1, 2) and protonated (3, 4) forms, *trans*-isomers (1, 3) and *cis*-isomers (2, 4).

Since the *cis*-isomer has a twisted nonplanar conformation, where the conjugation between the pyrene and quinoline nuclei through the ethylene group is partially broken, the local pyrene transitions in the *cis*-isomer are more pronounced than in the *trans*-isomer, hence the spectrum of the *cis*-isomer is more structured with additional maxima at 346 nm and 330 nm (Fig. 1, spectrum 2).

On comparing the spectra of the neutral and protonated species (Fig. 1) the position of the local pyrene absorption bands in the region of 330–350 nm is practically independent of the charge of the quinoline nucleus (0 or +1), while for the LWAB, characterizing the entire conjugated π-system, a significant bathochromic shift in the cationic form is observed to the region of 390–560 nm with maxima at 475 nm for the *trans*-isomer and 444 nm for the *cis*-isomer, (Fig. 1, spectra 3 and 4).

The neutral *E*-1P2QE fluoresces with a quantum yield of φ_{fl} = 0.28 and maximum at 476 nm, the fluorescence lifetime is 1.33 ns (Fig. S4†). On protonation, a bathofloric shift of the emission band to 591 nm and a decrease in intensity by more than an order of magnitude (φ_{fl} = 0.013) are observed.

Like many DAEs, 1P2QE can exist as s-*cis* or s-*trans* conformers (rotamers) relative to the single bond between the ethylenic group and quinoline nucleus.[31] The small dependence of the *E*-1P2QE fluorescence spectrum on the excitation wavelength (Fig. S5†) indicates the presence of different conformers in the solution. The conformers have slightly different spectral properties, while mono-exponential fluorescence decay implies that the conformers appear to have the same lifetime.

According to B3LYP/6-31G* calculations, in the ground S_0 state, the *E*-1P2QE s-*trans* conformer is higher in energy than the s-*cis* conformer by 0.98 kcal mol^{-1} (in vacuum); in ethanol (polarizable continuum model, PCM), the difference decreases to 0.67 kcal mol^{-1}. B3LYP/6-31G* predicts that the pyrene nucleus in the s-*cis* conformer is slightly twisted from the molecule plane (by ~22°), while PM3 predicts a planar structure (Fig. S6†). The *cis*-isomer is higher in energy than the *trans*-isomer by 6.30 kcal mol^{-1} for the s-*cis* conformer and 4.19 kcal mol^{-1} for the s-*trans* conformer (B3LYP/6-31G* data).

The frontier molecular orbitals, HOMO and LUMO, are delocalized along the entire conjugated molecule for both the s-*trans*- and s-*cis* conformers of 1P2QE. As an example, Fig. 2 shows the structure of the frontier MOs for the s-*cis* conformer; the same MOs for the s-*trans* conformer are shown in Fig. S7.† We can observe that for both s-*cis* conformers, HOMO is bonding with respect to the central ethylenic bond, while LUMO is antibonding with respect to this bond (Fig. 2 and Fig. S7†). A predominant localization of HOMO, particularly for the *cis*-isomers, can also be noted at the pyrene nucleus, where the HOMO structure corresponds to that of unsubstituted pyrene. According to the TDDFT calculations at the B3LYP/6-31G* level, the LWAB corresponds to the $S_1 \leftarrow S_0$ exci-

Open Access Article. Published on 08 December 2017. Downloaded on 1/20/2026 5:10:44 AM.
This article is licensed under a Creative Commons Attribution 3.0 Unported Licence.

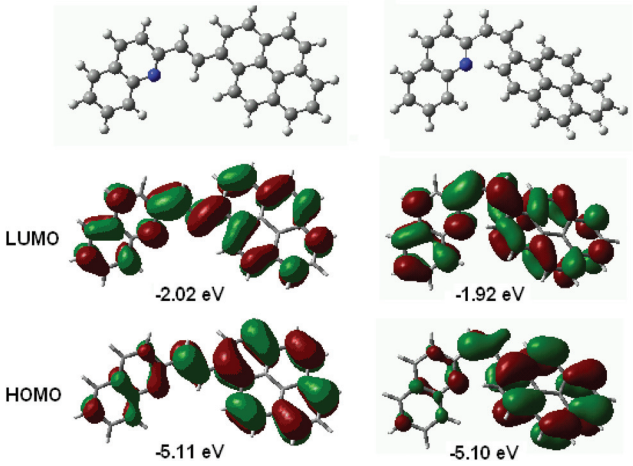

Fig. 2 Structure and energy of the frontier molecular orbitals for the s-*cis* conformer of *E*-1P2QE (left) and *Z*-1P2QE (right) calculated at the B3LYP/6-31G* level.

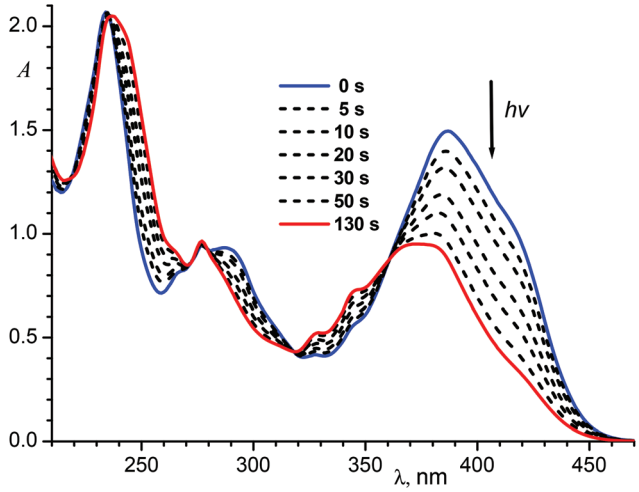

Fig. 3 Spectral variations during irradiation of an air-saturated solution of *E*-1P2QE (3.8×10^{-5} M) in ethanol with 405 nm light, intensity 4.1×10^{-9} Einstein cm^{-2} s^{-1}; the final spectrum corresponds to the photostationary state PS_{405}.

tation with exclusively (98%) HOMO → LUMO transition for both the s-*trans*- and s-*cis* conformers of 1P2QE (Table S1†). The calculated electronic absorption spectrum reproduces the experimental spectrum though the intensity of the $S_1 \leftarrow S_0$ transition is overestimated (Fig. S8†).

In the relaxed S_1 state, according to both semiempirical and DFT methods, the *E*-1P2QE adopts a planar structure (Fig. S9†). The single bonds between the ethylenic group and the aromatic nuclei shorten by ~0.03 Å, while the ethylenic double bond elongates by the same amount. This is a consequence of the electron transition from the bonding (with respect to the ethylenic bond) HOMO to the antibonding LUMO (Fig. 2 and Fig. S7†). Depopulation of the bonding MO and occupation of the antibonding MO weakens the ethylenic bond and is a prerequisite to π-bond rupture and rotation of the molecule fragments around the new single bond that can give rise to isomerization. Thus, results of the quantum-chemical calculations – the same MO structure and the same nature of the absorption band – predict the same photochemical properties for both *s*-conformers.

Upon irradiation of the *E*-1P2QE with visible light, we observed a fast reaction with spectral changes that corresponded to those for the *trans–cis* photoisomerization: decrease in the intensity and blue shift of the LWAB (Fig. 3). Observation of several isosbestic points at 218.4, 235.4, 279.2, 317.7 and 360.6 nm corresponded to the fact that only one reaction, namely, reversible photoisomerization, took place (Scheme 2). Principal component analysis gave a straight line with all points lying between *E*-1P2QE and *Z*-1P2QE (Fig. S10†), which corroborated the presence of only these two isomers in solution (though every isomer can exist as an equilibrated mixture of several *s*-conformers with a constant concentration ratio).

The spectral changes ceased on achieving the photostationary state (PS). The PS_λ composition depends on the irradiation

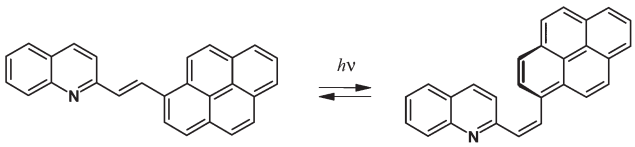

Scheme 2 Reversible photoisomerization of 1P2QE (on the example of the s-*trans* conformer).

wavelength λ and is defined through the relative content of the *cis*-isomer:

$$\eta_\lambda = [cis]_{PS_\lambda}/([trans]_{PS_\lambda} + [cis]_{PS_\lambda}), \quad (1)$$

where $[cis]_{PS_\lambda}$ and $[trans]_{PS_\lambda}$ are the concentrations of the *cis*- and *trans*-isomers in the PS_λ mixture, respectively. When a *trans*-isomer is the starting reactant, the parameter η_λ is the degree of conversion. Using two PSs, formed by irradiation with light of different wavelengths (PS_{405} and PS_{436}), as well as the *trans*-isomer spectrum, the *cis*-isomer spectrum was calculated by Fischer's method (Fig. 1, spectrum 2).

Investigation of the luminescent properties of the PSs enabled us to obtain information about the photoisomerization reaction mechanism. For the earlier studied SP, it is known that the *cis*-isomer possesses fluorescence and partly emits as the *trans*-isomer, which is adiabatically formed from the *cis*-isomer.[20] To examine the emitting properties of the 1P2QE *cis*-isomer, we investigated the luminescence spectra of different PSs as well as their luminescence excitation spectra. In all cases, the PSs spectra corresponded to the *trans*-isomer spectra (see an example in Fig. 4).

The luminescence intensity decreased linearly with increasing proportion of the *cis*-isomer in the PS (Fig. 5). The dependence was fitted by a linear regression, $I/I_0 = (1.002 \pm 0.007)$–

This journal is © The Royal Society of Chemistry and Owner Societies 2018

Open Access Article. Published on 08 December 2017. Downloaded on 1/20/2026 5:10:44 AM.
This article is licensed under a Creative Commons Attribution 3.0 Unported Licence.

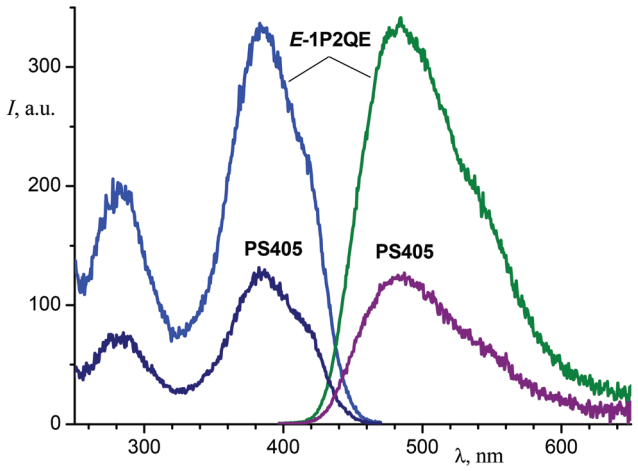

Fig. 4 Luminescence (right, excitation at 387 nm) and luminescence excitation (left, observation at 480 nm) spectra of *E*-1P2QE and the photostationary state PS_{405} (ethanol).

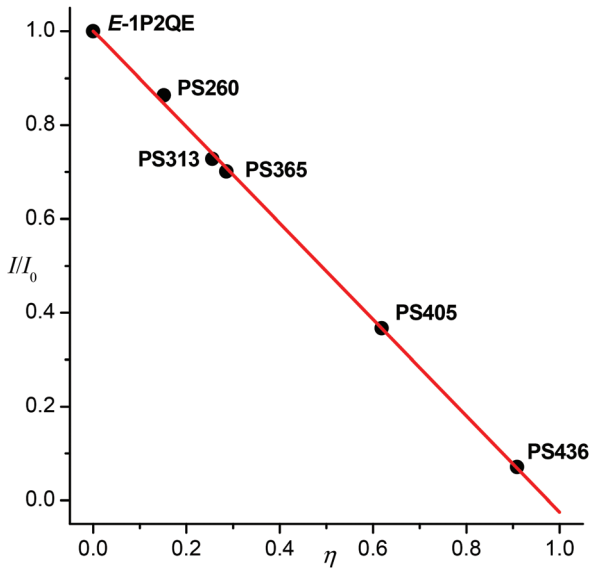

Fig. 5 Relative luminescence intensity of photostationary states is dependent on the PS composition (relative quantity of the *cis*-isomer η, see text).

$(1.027 \pm 0.015)\eta$, with correlation coefficient $R = -0.9996$. Therefore, the PS fluorescence is explained exclusively by the *trans*-isomer emission. The excited *cis*-isomer does not emit luminescence either by itself or through the excited *trans*-isomer that could be produced as a result of adiabatic isomerization of the former. The nonradiative processes in the excited *Z*-1P2QE (including the chemical reaction) prevail over the radiative deactivation.

Absence of the adiabatically formed *trans*-isomer means that the photoisomerization follows diabatic mechanism that implies existence of a minimum on the excited-state PES at the geometry of the *perp*-conformer, see below.

Calculations of the PES cross-sections reveal that the isomerization reaction profiles coincide with the conclusion based on the experimental data. Minimal energy paths of the rotation around the ethylenic double bond (dihedral angle β) in the ground (S_0) and lowest singlet-excited (S_1) states for the s-*cis* conformer are shown in Fig. 6; for the s-*trans* conformer, a similar picture was obtained (Fig. S11†).

In the ground state, two isomers, *trans*-(*E*) and *cis*-(*Z*), are separated by a high barrier at the *perp*-conformer geometry (β = 90°). The existence of the high ground-state barrier explains the absence of the thermal isomerization (at room temperature). On the excited-state PES, the *perp*-conformer corresponds to the minimum p^* (Fig. 6). After excitation, both *trans*- and *cis*-isomers achieve this minimum, and then, as a result of internal conversion (*via* conical intersection), the system relaxes to the ground-state maximum, where it can branch, with equal probability, between the *trans*- and *cis*-isomer; thus, the accepted value for the partitioning factor α is 0.5.[19,32,33] This corresponds to the diabatic mechanism of photoisomerization.

As mentioned above, protonation of the quinoline nitrogen atom results in the LWAB bathochromic shift that allows us to use visible light with wavelength up to 560 nm for the switching between different states of the molecule.

Fig. 7 shows spectral variations under exposure of the protonated *E*-1P2QE to the visible light. We observed a fast photoisomerization reaction similar to the neutral compound. Isosbestic points at 235.5, 282.1, 306.0 and 358.3 nm testified about the absence of side reactions. Spectral changes also ceased on achieving the PS; using two PSs (PS_{436} and PS_{546}) and the *trans*-isomer spectrum, the *cis*-isomer spectrum was calculated by Fischer's method (Fig. 1, spectrum 4).

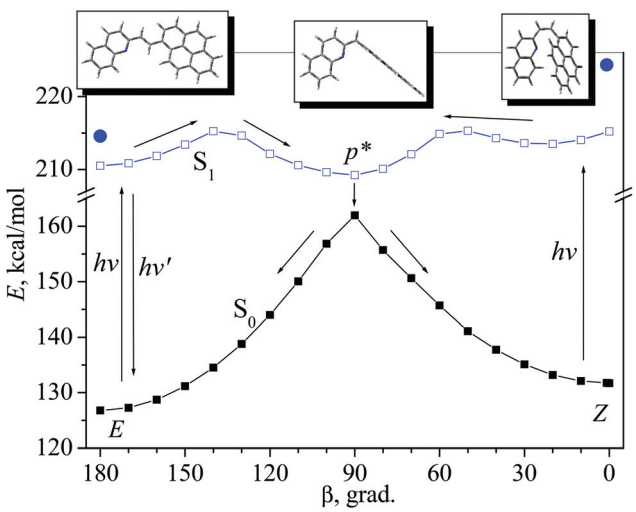

Fig. 6 Minimal energy paths of the isomerization reaction of the 1P2QE s-*cis*-conformer in the S_0 state (calculated by the PM3 method) and in the S_1 state (calculated by the PM3-CI(2 × 2) method); the arrows show the diabatic reaction path. The filled circles mark the location of the terms of the vertically excited isomers.

Open Access Article. Published on 08 December 2017. Downloaded on 1/20/2026 5:10:44 AM.
This article is licensed under a Creative Commons Attribution 3.0 Unported Licence.

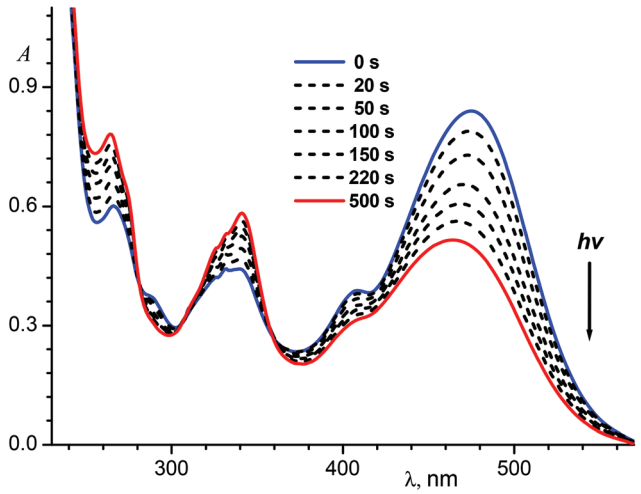

Fig. 7 Spectral variations during irradiation of an air-saturated solution of the hydrochloride *E*-1P2QE·HCl (2.5×10^{-5} M) in ethanol with 546 nm light; the final spectrum corresponds to the photostationary state PS_{546}.

The change in the kinetics of absorbance (A) for a reversible *trans–cis* photoisomerization is described by the differential eqn (2)

$$dA/dt = -(\varepsilon_t - \varepsilon_c) \cdot (\phi_{tc} \cdot A_t - \phi_{ct} \cdot A_c) \cdot (1-10^{-A}) \cdot I_0/A, \quad (2)$$

where ε_i and A_i are the molar absorption coefficient (MAC) and the absorbance of the isomer i at the irradiation wavelength, respectively, $A = \sum A_i$ is the total absorbance of the solution, and I_0 is the intensity of the incident light. The photoisomerization quantum yields are obtained by minimizing the squared difference between the experimental and calculated absorbance for all points, $\Delta A = (\sum(A_{calc} - A_{exp})^2/n)^{1/2}$, where A_{calc} is an absorbance calculated by numerical integration of eqn (2), A_{exp} is the measured absorbance, and n is the number of experimental points on the kinetic curve.[34] The following values were obtained: for the neutral 1P2QE, $\phi_{tc} = 0.23$ and $\phi_{ct} = 0.52$; for the protonated 1P2QE, $\phi_{tc} = 0.13$ and $\phi_{ct} = 0.83$.

The data obtained allow for the comparison of different pathways in the excited 1P2QE. The lifetime (τ) of the excited *E*-1P2QE (1.33 ns) is defined by the sum of the rate constants of three possible processes: fluorescence (k_{fl}), nonradiative decay (k_{nr}) and twisting to the *perp*-conformer (k_{tp}), $\tau = 1/(k_{fl} + k_{nr} + k_{tp})$. From $\varphi_{fl} = \tau k_{fl}$, we obtain $k_{fl} = 2.1 \times 10^8\ s^{-1}$. For diabatic photoisomerization, $\phi_{tc} = \alpha\tau k_{tp}$ and therefore, $k_{tp} = 3.5 \times 10^8\ s^{-1}$ and $k_{nr} = 1.9 \times 10^8\ s^{-1}$ (this can include internal conversion and intersystem crossing). Therefore, in the excited *E*-1P2QE, emission and nonradiative decay proceed with close efficiency, but chemical reaction is a main pathway. For *Z*-1P2QE, since $\varphi_{ct}/\alpha = 1.04$ (provided $\alpha = 0.5$, the theoretical limiting value is 1), chemical reaction is the only pathway for this isomer within an error of the quantum yield measurement. This explains the absence of the *cis*-isomer fluorescence.

The data for *E*-1P2QE can be compared with those for *E*-SP, which does not photoisomerize in the *trans* → *cis* direction (ϕ_{tc} ~0). The lifetime for the *E*-SP is 5.3 ns (hexane) and $\varphi_{fl} = 0.82$;[35] thus, $k_{fl} = 1.5 \times 10^8\ s^{-1}$ and $k_{nr} = 0.4 \times 10^8\ s^{-1}$.

Owing to effective photoisomerization, both neutral and cationic forms of 1P2QE can be used as molecular switches that are sensitive to visible light. However, it should be noted that for a molecular switch based on DAE *E*/*Z* isomerization, complete switching from one state to another is impossible because reversibility of the photoisomerization reaction and overlap of the isomer spectra prevent 100% conversion of one isomer to another upon exposure to light. As noted above, on irradiation with light of wavelength λ, a photostationary state PS_λ is achieved, whose composition is defined by a photostationary equilibrium condition (3).

$$(\varphi_{tc} \cdot \varepsilon_t \cdot [trans]_{PS})_\lambda = (\varphi_{ct} \cdot \varepsilon_c \cdot [cis]_{PS})_\lambda \quad (3)$$

According to condition (3), the lower the quantum yield, the greater is the concentration of the respective isomer in the PS. From eqn (3), we can obtain the dependence of the *cis*-isomer content in the PS on the irradiation wavelength (4).

$$\eta_\lambda = (\varphi_{tc} \cdot \varepsilon_t/(\varphi_{tc} \cdot \varepsilon_t + \varphi_{ct} \cdot \varepsilon_c))_\lambda \quad (4)$$

The variation of η_λ with λ enables us to estimate a range of possible switching abilities of any DAE as a molecular photoswitch.

The calculated curves for the neutral and protonated 1P2QE are shown in Fig. 8. For 1P2QE, the quantum yield ratio does not depend on the irradiation wavelength, so the dependence of η_λ on λ is defined exclusively by the MAC ratio $\varepsilon_t/\varepsilon_c$. The maximum η_λ dependence is observed at a wavelength where the $\varepsilon_t/\varepsilon_c$ ratio achieves a maximal value; conversely, the minimum on the η_λ dependence corresponds to the minimal $\varepsilon_t/\varepsilon_c$ value. Thus, for the neutral 1P2QE, the maximal (94%) and minimal (18%) content of the *cis*-isomer can be obtained at 441 nm and 251 nm, respectively (Fig. 8, curve 1).

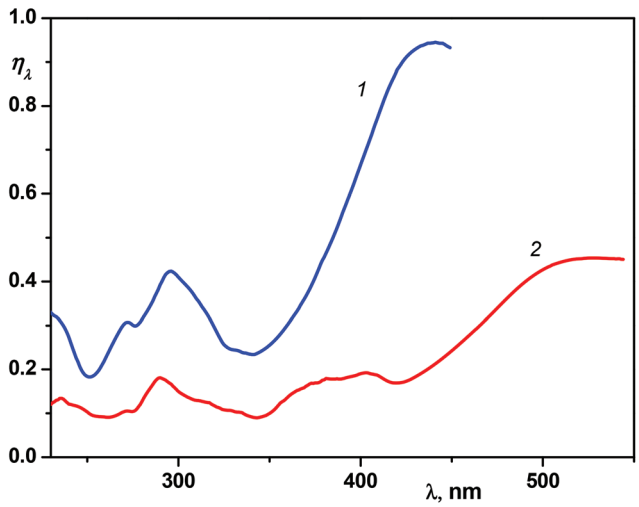

Fig. 8 Dependence of the photostationary state composition (relative quantity of the *cis*-isomer η_λ, see text) on the irradiation wavelength for the neutral (1) and protonated (2) 1P2QE.

 This journal is © The Royal Society of Chemistry and Owner Societies 2018

Open Access Article. Published on 08 December 2017. Downloaded on 1/20/2026 5:10:44 AM.
This article is licensed under a Creative Commons Attribution 3.0 Unported Licence.

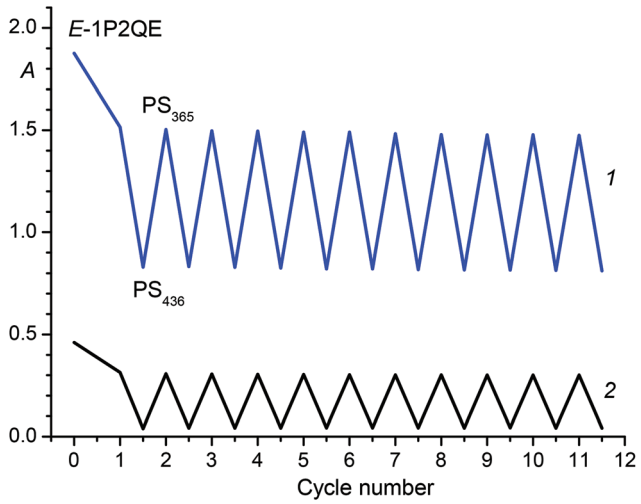

Fig. 9 Changes in absorbance upon alternating irradiation of an air-saturated solution of *E*-1P2QE in ethanol with UV (365 nm, 200 s) and visible (436 nm, 200 s) light: 1 – at 387 nm (the *E*-1P2QE absorption maximum), 2 – at 436 nm. High (low) absorbance corresponds to the photostationary state PS_{365} (PS_{436}).

A necessary property of a molecular photoswitch for application in optoelectronic devices is photostability with respect to side reactions. 1P2QE has high fatigue resistance. For example, Fig. 9 shows the changes in absorbance upon alternating irradiation with visible and UV light. The total time of irradiation was 4400 s, every cycle corresponded to the switching between two PSs: PS_{365} (η_{365} = 33%) and PS_{436} (η_{436} = 94%).

3. Conclusion

1-(1-Pyrenyl)-2-(2-quinolyl)ethylene (1P2QE) has a rather large conjugated π-system of 28 electrons. Nevertheless, it undergoes two-way reversible *trans* → *cis* and *cis* → *trans* photoisomerization with quantum yields as high as ϕ_{tc} = 0.23 and ϕ_{ct} = 0.52 for the neutral 1P2QE, and ϕ_{tc} = 0.13 and ϕ_{ct} = 0.83 for the protonated 1P2QE. For the neutral 1P2QE, both experimental data and quantum-chemical calculations testify the diabatic mechanism of photoisomerization. The neutral 1P2QE has a long-wavelength absorption band in the region of 340–460 nm with a maximum at 387 nm for the *trans*-isomer and 364 nm for the *cis*-isomer. Upon protonation, the absorption spectrum is red-shifted to 390–560 nm with a maximum at 475 nm for the *trans*-isomer and 444 nm for the *cis*-isomer. Due to high photoisomerization quantum yields and absorption in the visible region, 1P2QE can be used as a molecular photoswitch that is sensitive to visible light. The switching ability of 1P2QE is restricted by possible changes in the photostationary composition between the η_λ values (the *cis*-isomer content) in the range of 18–94% for the neutral form and 9–45% for the cationic form. To avoid possible deprotonation of the cationic form in basic media, the *N*-alkylated derivatives can be used.

Conflicts of interest

There are no conflicts of interest to declare.

Acknowledgements

This work was supported by the Russian Foundation for Basic Research (Grant No. 17-03-00789).

References

1 I. Rivalta, A. Nenov and M. Garavelli, Modelling retinal chromophores photoisomerization: from minimal models *in vacuo* to ultimate bidimensional spectroscopy in rhodopsins, *Phys. Chem. Chem. Phys.*, 2014, **16**, 16865–16879.
2 H. Kandori, Y. Shichida and T. Yoshizawa, Photoisomerization in Rhodopsin, *Biochemistry*, 2001, **66**, 1197–1209.
3 K. Szacilowski, Digital Information Processing in Molecular Systems, *Chem. Rev.*, 2008, **108**, 3481–3548.
4 M. F. Budyka, Molecular Photonic Logic Gates, *High Energy Chem.*, 2010, **44**, 121–126.
5 U. Pischel, J. Andreasson, D. Gust and V. F. Pais, Information Processing with Molecules - *Quo Vadis*?, *ChemPhysChem*, 2013, **14**, 28–46.
6 M. F. Budyka, Molecular switches and logic gates for information processing, the bottom-up strategy: from silicon to carbon, from molecules to supermolecules, *Russ. Chem. Rev.*, 2017, **86**, 181–210.
7 M. F. Budyka, N. I. Potashova, T. N. Gavrishova and V. M. Li, Design of Fully Photonic Molecular Logic Gates Based on the Supramolecular Bisstyrylquinoline Dyad, *Nanotechnol. Russ.*, 2012, **7**, 280–287.
8 M. F. Budyka and V. M. Li, Multifunctional Photonic Molecular Logic Gate Based On A Biphotochromic Dyad With Reduced Energy Transfer, *ChemPhysChem*, 2017, **18**, 260–264.
9 D. Bleger and S. Hecht, Visible-Light-Activated Molecular Switches, *Angew. Chem., Int. Ed.*, 2015, **54**, 11338–11349.
10 S. Helmy, F. A. Leibfarth, S. Oh, J. E. Poelma, C. J. Hawker and J. Read de Alaniz, Photoswitching Using Visible Light: A New Class of Organic Photochromic Molecules, *J. Am. Chem. Soc.*, 2014, **136**, 8169–8172.
11 X. Guo, J. Zhou, M. A. Siegler, A. E. Bragg and H. E. Katz, Visible-Light-Triggered Molecular Photoswitch Based on Reversible *E*/*Z* Isomerization of a 1,2-Dicyanoethene Derivative, *Angew. Chem., Int. Ed.*, 2015, **54**, 4782–4786.
12 S. Fredrich, R. Gostl, Ma. Herder, L. Grubert and S. Hecht, Switching Diarylethenes Reliably in Both Directions with Visible Light, *Angew. Chem., Int. Ed.*, 2016, **55**, 1208–1212.
13 T. van Leeuwen, J. Pol, D. Roke, S. J. Wezenberg and B. L. Feringa, Visible-Light Excitation of a Molecular Motor with an Extended Aromatic Core, *Org. Lett.*, 2017, **19**, 1402–1405.

Open Access Article. Published on 08 December 2017. Downloaded on 1/20/2026 5:10:44 AM.
This article is licensed under a Creative Commons Attribution 3.0 Unported Licence.

14 U. Mazzucato, Photophysical and photochemical behaviour of stilbene-like molecules and their aza-analogues, *Pure Appl. Chem.*, 1982, **54**, 1705–1721.
15 S. Malkin and E. Fischer, Temperature Dependence of Photoisomerization. III. Direct and Sensitized Photoisomerization of Stilbenes, *J. Phys. Chem.*, 1964, **68**, 1153–1163.
16 J. Saltiel, A. Marinari, D. W.-L. Chang, J. C. Mitchener and E. D. Megarity, Trans-Cis Photoisomerization of the Stilbenes and a Reexamination of the Positional Dependence of the Heavy-Atom Effect, *J. Am. Chem. Soc.*, 1979, **101**, 2982–2996.
17 A. Spalletti and G. Bartocci, Temperature and solvent effects on rotamer-specific photobehaviour of the *cis* and *trans* isomers of 2-styrylanthracene, *Phys. Chem. Chem. Phys.*, 1999, **1**, 5623–5632.
18 J. Saltiel, Y. Zhang and D. F. Sears Jr., Temperature Dependence of the Photoisomerization of *cis*-1-(2-Anthryl)-2-phenylethene. Conformer-Specificity, Torsional Energetics and Mechanism, *J. Am. Chem. Soc.*, 1997, **119**, 11202–11210.
19 M. F. Budyka, Diarylethene photoisometization and photocyclization mechanisms, *Russ. Chem. Rev.*, 2012, **81**, 477–493.
20 A. Spalletti, G. Bartocci, U. Mazzucato and G. Galiazzo, Decay pathways of the first excited singlet state of cis-1-styrylpyrene, *Chem. Phys. Lett.*, 1991, **186**, 297–302.
21 J. Zhou, X. Guo, H. E. Katz and A. E. Bragg, Molecular Switching via Multiplicity-Exclusive *E*/*Z* Photoisomerization Pathways, *J. Am. Chem. Soc.*, 2015, **137**, 10841–10850.
22 M. F. Budyka, N. I. Potashova, O. V. Chashchikhin, T. N. Gavrishova and V. M. Li, Photoisomerization of Naphthylquinolylethylenes in Neutral and Protonated Forms, *High Energy Chem.*, 2011, **45**, 492–496.
23 M. F. Budyka, N. I. Potashova, T. N. Gavrishova and V. M. Li, Photochemical Properties of 1-(9-Anthryl)-2-(2-Quinolyl)ethylene, *High Energy Chem.*, 2014, **48**, 185–190.
24 G. Drefahl, K. Ponsold and E. Gerlach, Untersuchungen über Stilbene, XXVII. Stilbazole mit höheren aromatischen Ringsystemen, *Chem. Ber.*, 1960, **93**, 481–485.
25 S. Ciorba, F. Fontana, G. Ciancaleoni, T. Caronna, U. Mazzucato and A. Spalletti, Fluorescence/photoisomerization competition in *trans*-aza-1,2-diarylethenes, *J. Fluoresc.*, 2009, **19**, 759–768.
26 V. M. Li, T. N. Gavrishova and M. F. Budyka, Microwave-Assisted Solvent-Free Synthesis of 2-Styrylquinolines in the Presence of Zinc Chloride, *Russ. J. Org. Chem.*, 2012, **48**, 823–828.
27 H. D. Becker, Unimolecular photochemistry of anthracenes, *Chem. Rev.*, 1993, **93**, 145–172.
28 M. J. Frisch, G. W. Trucks, H. B. Schlegel, G. E. Scuseria, M. A. Robb, J. R. Cheeseman, G. Scalmani, V. Barone, B. Mennucci, G. A. Petersson, H. Nakatsuji, M. Caricato, X. Li, H. P. Hratchian, A. F. Izmaylov, J. Bloino, G. Zheng, J. L. Sonnenberg, M. Hada, M. Ehara, K. Toyota, R. Fukuda, J. Hasegawa, M. Ishida, T. Nakajima, Y. Honda, O. Kitao, H. Nakai, T. Vreven, J. A. Montgomery Jr., J. E. Peralta, F. Ogliaro, M. Bearpark, J. J. Heyd, E. Brothers, K. N. Kudin, V. N. Staroverov, R. Kobayashi, J. Normand, K. Raghavachari, A. Rendell, J. C. Burant, S. S. Iyengar, J. Tomasi, M. Cossi, N. Rega, J. M. Millam, M. Klene, J. E. Knox, J. B. Cross, V. Bakken, C. Adamo, J. Jaramillo, R. Gomperts, R. E. Stratmann, O. Yazyev, A. J. Austin, R. Cammi, C. Pomelli, J. W. Ochterski, R. L. Martin, K. Morokuma, V. G. Zakrzewski, G. A. Voth, P. Salvador, J. J. Dannenberg, S. Dapprich, A. D. Daniels, O. Farkas, J. B. Foresman, J. V. Ortiz, J. Cioslowski and D. J. Fox, *Gaussian 09, Revision B.01*, Gaussian, Inc., Wallingford CT, 2010.
29 E. Fischer, The Calculation of Photostationary States in Systems A<=>B When Only A Is Known, *J. Phys. Chem.*, 1967, **71**, 3704–3706.
30 J. Duhamel, Internal Dynamics of Dendritic Molecules Probed by Pyrene Excimer Formation, *Polymers*, 2012, **4**, 211–239.
31 U. Mazzucato and F. Momicchioli, Rotational Isomerism in *trans*-1,2-Diarylethylenes, *Chem. Rev.*, 1991, **91**, 1679–1719.
32 V. D. Vachev, J. H. Frederick, B. A. Grishanin, V. N. Zadkov and N. I. Koroteev, Quasiclassical Molecular Dynamics Simulation of the Photoisomerization of Stilbene, *J. Phys. Chem.*, 1995, **99**, 5247–5263.
33 G. Bartocci, U. Mazzucato and A. Spalletti, The role of the adiabatic mechanism in the photoisomerization of 1,2-diarylethenes and related compounds, *Trends Phys. Chem.*, 2007, **12**, 1–36.
34 M. F. Budyka, N. I. Potashova, T. N. Gavrishova and V. M. Li, Photoisomerization of 2-Styrylquinoline in Neutral and Protonated Forms, *High Energy Chem.*, 2008, **42**, 446–453.
35 Y. Kikuchi, H. Okamoto, T. Arai and K. Tokumaru, Effects of solvents and substituents controlling the adiabatic or diabatic modes of the cis ->trans isomerization of styrylpyrenes in the excited singlet state, *Chem. Phys. Lett.*, 1994, **229**, 564–570.

 This journal is © The Royal Society of Chemistry and Owner Societies 2018